Model-Enhanced Localization of Forced Oscillation Using PMU Data

Bernard C Lesieutre
Deparment of Electrical and Computer Engineering
University of Wisconsin-Madison
Madison, USA
lesieutre@wisc.edu

Yasmine Abdennadher
Deparment of Electrical and Computer Engineering
University of Wisconsin-Madison
Madison, USA
abdennadher@wisc.edu

Sandip Roy
Deparment of Electrical and Computer Engineering
Washington State University
Pullman, USA
sandip@wsu.edu

***Abstract*—The detection and mitigation of low-frequency forced oscillations are important for reliable grid operation. Forced oscillations, driven by periodic disturbances such as malfunctioning controllers [1], may resonate with poorly-damped natural modes across wide areas of the grid, and risk large system failures. Locating the source within the system is a prerequisite for mitigation schemes to correct the actions responsible for the original oscillation. We introduce a model-enhanced method for locating the source of a forced oscillation using PMU measurements. This method augments the use of data-only approaches, such as the energy based function inspired dissipating energy flow method. The algorithms are tested on several scenarios using a 240-bus, 178-line WECC model.**

***Index Terms*—Power Systems, Forced Oscillations, Phasor Measurement Units**

I. Introduction

Low-frequency oscillations are related to the electromechanical swing dynamics of the power grid. Broadly, bulk power grid operators are concerned with persistent low-frequency electromechanical oscillations, primarily because they can lead to device failures and outages. These oscillations can be classified into two types: 1. free oscillations, and 2. forced oscillations. Free oscillations occur as the natural response to an impulsive event. They are typically caused by the dynamic interactions among different devices in a power grid [2]. Forced oscillations are typically driven by sinusoidal or periodic signals originating at generator sites [3]. These oscillations may resonate with poorly-damped natural modes across wide areas of the grid, and risk large system failures. Locating the source within system is a prerequisite for mitigating the actions responsible for the original oscillation.

Researchers have demonstrated that, given an oscillation event that is sufficiently strong and long lasting, detecting the event is straightforward. However, locating the source is more complicated because there are limited measurements and those measurements exhibiting the largest oscillations may occur distant from the source.

The majority of techniques that appear in the literature can be classified into three major categories. The damping torque method, mode shapes estimation based method, and energy based method. The damping torque method introduced and studied in [4]–[8] utilizes generator measurements to calculate the damping torque coefficient and mode for each generator in order to determine the oscillation source. The generator with a positive damping torque coefficient is believed to provide negative damping to the system, and therefore identified as the oscillation source [8].This method was initially introduced for a single machine infinite bus system (SMIB) in [4] and later on extended to a multi-machine system [5]. Despite its success in locating the source in a poorly damped oscillation case, the damping torque method was found to have trouble identifying forced oscillation sources [8]. Additionaly the authors found that in cases where the amplitude was too small the results were misleading.

The mode shape estimation method [8]–[12] derives the relative magnitude and phase of the oscillation throughout the system using mode shape estimation from phasor measurement units (PMU) measurements. [9] demonstrated that the generator with leading phase indicated less damping contribution, and is therefore the source of oscillation. Although this method located the right source in multiple test cases it may not necessarily help in locating all forced oscillations [12]. Additionally within the real power system, the mode shape method is hard to implement due to the inaccuracies in modeling [8].

Energy plays an important role in oscillations. The amount of energy within a region is related to the oscillation amplitude. Therefore, [13] used an energy flow model to detect and locate oscillation sources in power system. With energy being a primary attribute of oscillation, this method is seen to be more robust than others that utilize oscillation attributes such as magnitude, phase angle, and statistical signatures [14]. Through implementing this method it is shown that the oscillation source produces energy that is dissipated across the power system. Therefore, by calculating the energy flow within the system the oscillation can be traced and found. The method was further studied in real time operation in [14] and [15]. Despite the wide range of studies within the energy based method, recent findings in [16] demonstrated that the energy from devices in the system can change abruptly under

different forced oscillation frequencies. Such changes makes it difficult to locate the source of oscillation within diverse operating conditions.

In addition to the above methods, there have been other developed techniques to aid in locating the source of oscillation within the power grid. The majority of the methods introduced in [17]–[22] tend to depend on PMU measurements and the system model information. However, most of these methods have yet to be proven robust in differing scenarios.

The aim of this paper is to introduce a model enhanced approach to determine the oscillation source. This can be applied in practice along with data-only method such as the dissipating energy flow model [13]. The remainder of the paper is organized as follows. Section II will describe the model enhanced approach, the particular issues that were faced, and a summary of the energy based method. Section III implements both methods on NASPI case studies motivated by the WECC system [23]. Finally. section IV summarizes the paper and propose any future work.

II. Approach

A. Model Enhanced

The model-enhanced approach attempts to match observations of forced oscillations to oscillations predicted by a model. The observations are represented as complex phasors at the frequency of the oscillation. The model must capture system dynamics at the frequency of oscillation from which comparative phasors may be computed. Power system dynamics model are typically represented as a set of nonlinear differential/algebraic equations:

$$\frac{dx}{dt} = f(x, y, u) \tag{1}$$

$$0 = g(x, y, u) \tag{2}$$

$$z = h(x, y, u) \tag{3}$$

where x are dynamic variables, y are algebraic variables, u represents inputs, and z are outputs to match to the measurements. Assuming that the model is accurate and known, it can be used to calculate the response to forced oscillations, simply by applying a forced oscillation at each input. In practice forced oscillations typically arise from a single driving force at one location.[1] Exhaustively applying an oscillatory signal at each input and matching the results of the simulations to the observations should reveal the source of the oscillation.

This exhaustive simulation-based approach is conceptually straight-forward but time consuming and unnecessary. Using a linearized model and frequency-domain phasor analysis, the effect of each input can be computed directly from the model using algebraic techniques. Specifically we can easily compute the transfer function from input to output at the desired frequency. Using Laplace transforms the linearized model of (1)-(3) takes the form

$$\begin{bmatrix} sX(s) \\ 0 \\ Z(s) \end{bmatrix} = \begin{bmatrix} F_x & F_y \\ G_x & G_y \\ H_x & H_y \end{bmatrix} \begin{bmatrix} X(s) \\ Y(s) \end{bmatrix} + \begin{bmatrix} F_u \\ G_u \\ H_u \end{bmatrix} U(s) \tag{4}$$

This model (4) can be reduced to obtain a multi-input, multi-output transfer function as a function of frequency, $Z(s) = H(s)U(s)$. From the measurements, we estimate the frequency of the oscillation. Let us denote this frequency as f_{osc}. For high-order systems, it is simpler to substitute $s = j2\pi f_{osc}$ in (4) prior to the reduction. In either case, at the frequency of oscillation we easily compute the relation between input phasors and output phasors at the frequency of oscillation:

$$Z(f_{osc}) = H(f_{osc})U(f_{osc}) \tag{5}$$

Assuming that there is a single source for the forced oscillation, the location of the source can be determined by finding the column of $H(f_{osc})$ that is most aligned with the measurement Z_{meas}. Note that the amplitude and phase of the input are unknown. To perform the comparison, the columns of $H(f_{osc})$ can first be normalized to best match the amplitude and phase of an elements of Z_{meas} (or vice-versa). Specifically, we compute the $U_i(f_{osc})$ that best fits the measurement for each single location scenario:

$$Z_{osc,i} = H_{osc,i}U_i \approx Z_{meas} \tag{6}$$

where $H_{osc,i}$ is the ith column of $H(f_{osc})$, and U_i is the least-squares solution of $H_{osc,i}U_i = Z_{meas}$. Best alignment is determined by largest value of the normalized inner products of the measurement vector and the model-computed measurement vectors, each calculated as

$$\Re\left(\frac{Z_{osc,i}^H Z_{meas}}{|Z_{osc,i}||Z_{meas}|}\right) \tag{7}$$

1) Practical Issues: There are several practical issues that complicate the direct application of the ideal approach outlined above. These include

- Model (1)-(3) may not be perfect and the extent of inaccuracies will need to be investigated. It is desireable that the method will provide a result that is in the neighborhood of the actual location. Inaccuracies can be due to unknown differences between the model and the true system, and to a lesser extent the use of a linearized model instead of a nonlinear model.
- The method is intended to be applied to industry models and yet there appear to be no commercial tools that will compute the linearized model in the form described above in (4). Below we discuss how we adapt the linearized model from a commercial product to meet our needs.
- The measurements are not accurate. In particular, voltages and currents estimated from phasor measurements may have biases due to sensor readings and PMU filtering. We will propose a coarse way to partly mitigate this potential issue through a generic phase shift.

[1] In theory it is possible to have multiple sources of forced oscillations at the same frequency, and the analysis would need to be more sophisticated.

- The results may not uniquely identify a single source with confidence. Instead, a number of buses in a region may stand out as nearly indistinguishable by the correlation method.

With regard to the accuracy of the model, we proceed here assuming that the given model is free of fundamental inaccuracies. Later we can perform sensitivities studies to assess the fidelity of the model.

To address the issue of obtaining a linearized model for industry models, we adapt the model available from the PowerTech DSA set of tools (PSAT, TSAT, SSat) [24]–[26]. These tools are used to assess power system stability via simulations, eigenanalysis, and participation factors. The linearized model the program makes for this purpose is available to user and takes the form [24]–[26]

$$\frac{dx}{dt} = Ax + By \tag{8}$$

$$0 = Cx + (D - Y_{bus})y \tag{9}$$

The A, B, C, D, and Y_{bus} matrices are computed by the program; x are dynamic variables, and the algebraic variables, y, are specifically the bus voltages in rectangular coordinates. The algebraic equations represent the current balance at each bus. All generator internal algebraic equations are reduced out, and the loads are converted to impedances.

This model appears close to what we need, however, it doesn't include any inputs. Without knowledge of the internal workings of the program (and perhaps with) it is difficult to augment the model to include inputs for voltage set-point, or power set-point, or any other specific inputs. Instead, we introduce current injections at each bus, and treat these as the inputs. As an oscillation of one of the actual inputs will impact the current injected into the grid, these external current injections serve as proxies for those inputs, and can serve to locate the source of the oscillation. The measurements we consider can all be expressed in terms of the bus voltage phasors. These include bus voltages and line currents. The augmented model we use can be expressed as

$$\frac{dx}{dt} = Ax + By \tag{10}$$

$$u = Cx + (D - Y_{bus})y \tag{11}$$

$$z = H_y y \tag{12}$$

As before, these equations can be algebraically reduced using frequency-domain methods to obtain a transfer model of the form $Z(s) = H(s)U(s)$ which we evaluate at the frequency of the forced oscillation, f_{osc}.

The third practical issue we address here has to do with imperfect, biased measurements. The measurements are presumed to come from Phasor Measurement Units (PMUs) which themselves rely on voltage and current sensors. There are several potential sources of errors including phase introduced by current transducers and by the subsequent filtering by the PMU. Likewise, magnitude calculations may also be affected. A detailed approach to modeling all the measurements devices is unweildly and impractical. A simpler approach recognizes that measurements may include errors, particularly in phase, and to compensate for this unknown factor. In this paper we do this generically by applying a common uniform phase error in current measurements. This complicates our algorithm by necessitating a one-dimensional search over values of compensating phase in the measurements to best match to the computed model-based phasors. The compensated measurements $I_{line,c}$ with compensating phase ϕ_c are given by

$$I_{line,c} = I_{line} e^{j\phi_c} \tag{13}$$

where I_{line} corresponds to the subset of measurements Z_{meas} associated with line current measurements.

Finally, the results of this approach may yield correlations that are very close, making it difficult to distinguish a single source, at least as viewed from the given measurements. If the model is presented in very fine detail, it is possible that a forced oscillation introduced at neighboring buses could yield a very similar response in the measurements. In such cases a metric will need to be developed to robustly identify a set of buses from which the oscillation may originate.

B. Data based

There are a number of methods for locating the source of a forced oscillation using only measurements. The first method is to infer a region from the location of the largest voltage and line current oscillations. This approach is not reliable especially when the frequency of oscillation is near to a natural mode of the system. An extension of this approach looks at the strength of harmonics of the forced oscillations, which are present in many events. The strength of higher harmonics will decrease rapidly with distance from the source of oscillation [22]. This is helpful in cases when harmonics are observed. Another approach is motived by energy-based analysis. This approach calculates Dissipating Energy flow in branches, which should flow from the source of oscillation.

The energy-based method [13] calculates the dissipated energy flow within each branch in the network, and demonstrates that the resulting energy is related to the energy dissipated by the damping torque. This method was first introduced in [13] and further developed in [14]. In both papers, the authors derive the dissipating energy within each line by utilizing power and polar coordinates. In implementing this method we found it more convenient to derive the energy using the current and the voltage at each bus formulation shown in [13] and in (14).

$$W = \int \mathrm{Im}(\mathrm{I}_{\mathrm{ij}}^{*}\mathrm{dU_i}) = \int (I_{ij,x} dV_{i,y} - I_{ij,y} dV_{i,x}) \tag{14}$$

From the PMU measurements we can obtain each monitored device's voltage and current magnitude and angle. Given PMU measurements we can compute the voltage and current quantities as a function of time (15)-(18) within each monitored line and bus:

$$I_{ij,x} = I_{ij,x0} + I_{ij,x1}\cos(\omega t + \phi_{x1}) \quad (15)$$
$$I_{ij,y} = I_{ij,y0} + I_{ij,y1}\cos(\omega t + \phi_{y1}) \quad (16)$$
$$V_{i,x} = V_{i,x0} + V_{i,x1}\cos(\omega t + \theta_{x1}) \quad (17)$$
$$V_{i,y} = V_{i,y0} + V_{i,y1}\cos(\omega t + \theta_{y1}) \quad (18)$$

Given that we have these quantities as a function of time, we can then express the integral (14) as a function of time as well:

$$W = \int \mathrm{Im}(\mathrm{I}_{\mathrm{ij}}^{*}\mathrm{dU_i}) = \int (I_{ij,x}dV_{i,y} - I_{ij,y}dV_{i,x}) = \int (I_{ij,x}\frac{dV_{i,y}}{dt} - I_{ij,y}\frac{dV_{i,x}}{dt})dt \quad (19)$$

Which then expands to:

$$\begin{aligned} W = &\int \left(-\omega\frac{I_{ij,x1}V_{i,y1}}{2}\sin(\theta_{y1} - \phi_{x1})\right) \\ &+ \left(\omega\frac{I_{ij,y1}V_{i,x1}}{2}\sin(\theta_{x1} - \phi_{y1})\right)dt \\ &+ \int (-\omega I_{ij,x0}V_{i,y1}\sin(\omega t + \theta_{i,y1}) \\ &+ (\omega I_{ij,y0}V_{i,x1}\sin(\omega t + \theta_{i,x1}))\,dt \\ &+ \int \left(-\omega\frac{I_{ij,x1}V_{i,y1}}{2}\sin(2\omega t + \theta_{y1} + \phi_{x1}\right) \\ &+ \left(\omega\frac{I_{ij,y1}V_{i,x1}}{2}\sin(2\omega t + \theta_{x1} + \phi_{y1})\right)dt \end{aligned} \quad (20)$$

When integrated over one period, we find that the second and third term of (20) integrate to zero. Throughout the time window, the only term that contributes to this integral in the long term is the constant term within (20):

$$\begin{aligned} DW = &-\omega\frac{I_{ij,x1}V_{i,y1}}{2}\sin(\theta_{y1} - \phi_{x1}) \\ &+\omega\frac{I_{ij,y1}V_{i,x1}}{2}\sin(\theta_{x1} - \phi_{y1}) \end{aligned} \quad (21)$$

The DW term is understood to be the average Dissipating Power, and is used to identify the direction of Dissipating Energy Flow due to a sustained oscillations. Its value can also be expressed in terms of phasor quantities associated with the oscillations. The rms phasors can be associated as follows:

$$I_x = \sqrt{2}I_{ij,x}e^{j\phi_x} \leftrightarrow I_{ij,x1}\cos(\omega t + \phi_{x1}) \quad (22)$$
$$I_y = \sqrt{2}I_{ij,y}e^{j\phi_y} \leftrightarrow I_{ij,y1}\cos(\omega t + \phi_{y1}) \quad (23)$$
$$V_x = \sqrt{2}V_{i,x}e^{j\theta_x} \leftrightarrow V_{i,x1}\cos(\omega t + \theta_{x1}) \quad (24)$$
$$V_y = \sqrt{2}V_{i,y}e^{j\theta_y} \leftrightarrow V_{i,y1}\cos(\omega t + \theta_{y1}) \quad (25)$$

Using the phasor quantities (22)-(25), the dissipating power from 21 can be concisely expressed as:

$$DW = \omega\ \mathrm{Im}(\mathrm{V_x I_y^{*}} - \mathrm{V_y I_x^{*}}) \quad (26)$$

This expression is used in our analysis in the next section.

III. Results

The model-enhanced and data-only methods described in Section II are applied to a 243-bus, 178-branch power model motivated by the WECC system [23]. This model was adapted for use in the 2021 IEEE-NASPI Oscillation Source Location Contest [23]. Thirteen forced-oscillation scenarios were created for the contest by varying the model and applying different disturbances. These disturbances were designed to be difficult; the frequency of the forced oscillation was chosen to resonate with natural modes, and faults were applied during the forced oscillation in order to excite the natural modes. In this paper we report on the application of these methods to the first four scenarios used in the contest. The specific features of the scenarios are described in the results key for the event [23], and we summarize those here:

- Scenario 1. A 0.82 Hz forced Oscillation is applied to the governor of a generator located at bus 1431.
- Scenario 2. A 1.19 Hz forced oscillation is applied to the governor of a generator located at bus 2634.
- Scenario 3. A 0.379 Hz forced oscillation is applied to the exciter of a generator located at bus 1131.
- Scenario 4. A 0.379 Hz forced oscillation is applied to the governor of a generator located at bus 3831.

Scenarios 2,3 and 4 all have a forced oscillation that resonates with a natural mode, and also involve an applied fault to excite those modes.

In our analysis we use the data supplied with the IEEE-NASPI contest [23]. The data are supplied as time-series samples of voltage magnitude and angle at 58 buses, and line current magnitude and angle at 89 lines. We process this data to estimate the frequency of the forced oscillation, and to represent the rectangular coordinate components of the monitored complex voltages and line currents as phasors at the frequency of the forced oscillations;, i.e., V_x, V_y, I_x, I_y. These are inputs into our methods.

A. Model-Enhance Results

The linearized model used in this approach is obtained using the steps described in Section II. The SSAT tool was used to obtain a linearized model (8)-(9) from the nonlinear model for each scenario. Because this model doesn't contain explicit inputs, we applied proxy current induction inputs at each bus, and added output relations corresponding to measurements to obtain a model in the form (10)-(12). Using this model, we calculate the transfer function at the oscillation frequency and compute the predicted output phasor profile associated with each input. We repeat this by varying a uniform compensating phase in the line current measurements noted in (13). The alignment of each predicted phasors to the compensated measured phasors is computed using (7).

The results are summarized in Table I in which the two buses with the highest correlations are displayed. In each scenario, the correct bus is identified as the source. In Scenario 1 and Scenario 2, the correct source stands out with a relatively large gap in the correlation values. In these two cases the line

TABLE I
THE CANDIDATE SOURCES WITH THE TWO HIGHEST CORRELATION VALUES FOR EACH SCENARIO.

Scenario 1: $f_{osc} \approx 0.815$	
correlation	Bus
0.7149	1431
0.5977	1401
Scenario 2: $f_{osc} \approx 1.189$	
correlation	Bus
0.7121	2634
0.6732	2604
Scenario 3: $f_{osc} \approx 0.381$	
correlation	Bus
0.7264	1131
0.7264	1101
Scenario 4: $f_{osc} \approx 0.384$	
correlation	Bus
0.7243	3831
0.7243	3801

current compensating phase (7) did affect the value of the correlations but did not affect the end results; the same bus was identified as the source. In Cases 3 and 4 there are many candidate sources with similar correlation values. While the correct bus had the highest correlation in both cases, there are multiple buses with nearly equal correlations. For Scenario 3, there are 9 other buses with correlations within 1% of the maximum value, in scenario 4, there are 20 other buses with correlations within 1% of the maximum value. All are in the immediate vicinity of the correct source. In both of these scenarios the compensating phase value did impact the results. The phase compensation for Scenarios 3 and 4 are 1.32 and 4.65 degrees respectively. These gave the highest possible correlation value in each case. For Cases 3 and 4 it will be useful to apply an appropriate metric to identify a regional set of buses that will include the true source.

The ability, or inability, to distinguish between potential sources of forced oscillations is a property of the system, the frequency of the oscillations, and the measurements. To examine this system property, we propose determining how close two measurements can be, produced by driving oscillations at two different buses. We then apply this calculation exhaustively, pairwise, for each bus. Specifically we pose the problem

$$\min_{U_m, U_n} |Z_m - Z_n|_2 \tag{27}$$

$$\text{s.t.} \quad |U_m|_2 = 1 \tag{28}$$

where Z_m and Z_n are the measurements produced by forcing oscillations U_m and U_n at buses m and n respectively. Using the transfer function relating inputs to outputs, this optimization problem can be written as

$$\min_{U_m, U_n} \begin{bmatrix} U_m^T & U_n^T \end{bmatrix} \left[\begin{bmatrix} H_m^T \\ -H_n^T \end{bmatrix} \begin{bmatrix} H_m & -H_n \end{bmatrix} \right] \begin{bmatrix} U_m \\ U_n \end{bmatrix} \tag{29}$$

$$\text{s.t.} \quad \begin{bmatrix} U_m^T & U_n^T \end{bmatrix} \begin{bmatrix} I & 0 \\ 0 & 0 \end{bmatrix} \begin{bmatrix} U_m \\ U_n \end{bmatrix} = 1 \tag{30}$$

where H_m and H_n are the transfer functions relating the inputs at buses m and n to the output measurements. Note that without loss of generality, we make these computations using real variables and parameters, expanding the complex equations and variables into real and imaginary parts.

The first-order optimality conditions for this optimization problem are

$$\left[\begin{bmatrix} H_m^T \\ -H_n^T \end{bmatrix} \begin{bmatrix} H_m & -H_n \end{bmatrix} \right] \begin{bmatrix} U_m \\ U_n \end{bmatrix} = \lambda \begin{bmatrix} I & 0 \\ 0 & 0 \end{bmatrix} \begin{bmatrix} U_m \\ U_n \end{bmatrix} \tag{31}$$

$$\begin{bmatrix} I & 0 \\ 0 & 0 \end{bmatrix} \begin{bmatrix} U_m \\ U_n \end{bmatrix} = 1 \tag{32}$$

which is a generalized eigenvalue problem. Reducing out the U_n variables, this can be further simplified to a standard eigenvalue problem. The solutions of (31)-(32) for U_m and U_n enable the calculation of minimum error (or closeness) of two measurements driven by oscillations from different sources, as posed in (27). By repeated calculation for each bus, we can identify other bus locations that may yield nearly identical measured outputs. For comparison we use a normalized error:

$$\frac{|Z_m - Z_n|_2}{|Z_m|_2} \tag{33}$$

We apply this method to our different test cases. For Case 1 and source bus 1431 (index 7), we show the normalized errors in Figure 1. The bus index with the lowest normalized error is index 7, bus 1431 itself. No other bus is very close, indicating that a source at that bus should be easily distinguished, consistent with our test case. For the results for case 4 using bus 3831 (index 24), shown in Figure 2, there are many buses with very low normalized errors, suggesting that this source is hard to distinguish from others for the particular frequency of oscillation and given measurements. This result is also consistent with our analysis of this test case.

B. Dissipating Energy Flow Results

The results of the energy flow method were obtained using the steps described in Section III-A. Using the computed phasors (22)-(25) for the monitored lines and buses, we determine the the dissipated power (21) within each branch for the same four scenarios.

Figure 3 demonstrates the dissipating power within case 1. Thicker arrows represent higher magnitude power flow while thinner arrows represent lower magnitude power flow. Given that the oscillation occurs at the generator in bus 1431, we see that larger sources of power were concentrated in nearby lines. Specifically in lines 1431-1401, 1401-1402, and 1402-1301 which are directly or maximum two steps away from

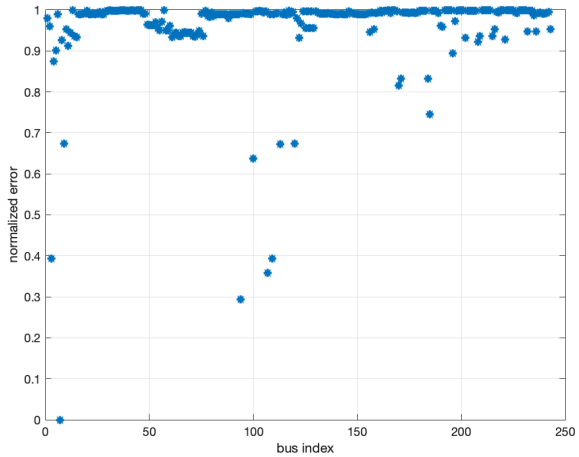

Fig. 1. Normalized error for pairwise bus comparisons with bus 1431 (index 7).

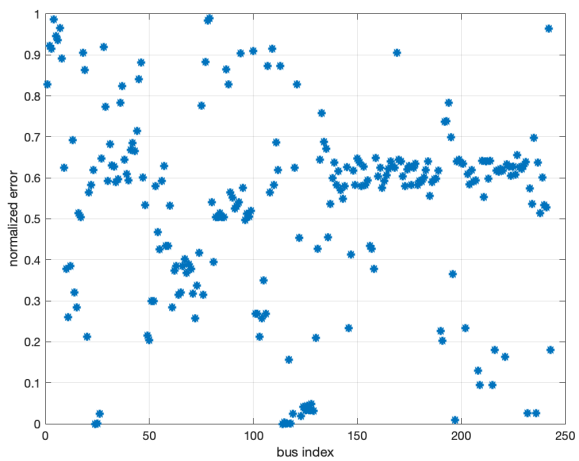

Fig. 2. Normalized error for pairwise bus comparisons with bus 3831 (index 24).

the source of oscillation. Additionally, the figure demonstrates that in most cases the energy is flowing away from the source and towards neighboring generator buses. This result satisfies the hypothesis that given an oscillation at a certain bus, the energy would flow away from the source.

Implementing the same method on Cases 2-4 we were able to obtain similar results. Table II demonstrates the location of each source and highlights the three top lines within each case that had the highest magnitude of power. In case 2 the results demonstrated that the dissipating energy was going away from the bus 2634 and towards near by generation buses. Although hidden from the case map [23], the line connected to the oscillation source had the highest magnitude as conveyed in table II. At 30 seconds the natural mode was excited by the fault at bus 1131. Despite this interruption in the system, the results still demonstrated the highest dissipating energy to be flowing away from the forced oscillation source, bus 2634.

TABLE II
THE BRANCHES WITH THE HIGHEST DISSIPATED POWER FOR EACH CASE

Case Number	Oscillation Source	Frequency (Hz)	Lines with Highest DW
Case 2	2634	1.19	2634 - 2604 6503 - 2533 2604 - 6504
Case 3	1131	0.379	1201 - 2901 2408 - 2438 1402 - 1301
Case 4	3831	0.379	2404 - 2401 2901 - 1201 2401 - 2603

Unlike the previous two cases, scenarios 3 and 4 had some limitations. Both cases experienced forced oscillations distant from directly monitored lines and buses. Therefore, it was more challenging to draw a concrete conclusion. Looking at the monitored lines in cases 3 and 4 it appeared that the energy was mostly dissipating away from the source. Similarly to case 2, case 3 experienced a natural oscillation in bus 2503 at 30 seconds. Unlike case 2, there seemed to be higher dissipating energy closer to this fault, which added another level of complexity in determining the source of oscillation.

IV. CONCLUSION

In this paper we pursue a model-enhanced method for determining the source of a forced oscillation that is based on the premise that a very accurate model can be probed with an exhaustive set of inputs to match simulations to measurements. This approach becomes computationally feasible with the use of a linearized model to directly compute the relation between input phasors and output phasors without simulation. In application we adapted an industry tool to obtain the linearized model with proxy current injection inputs at each bus. We addressed another practical issue by compensating the phase of the line current measurements. The results are promising in that model-based approach correctly identified the source of the forced oscillation in each of the four scenarios we studied. We anticipate that this model-enhance approach will augment data-only methods such as the dissipating energy flow method, which can be limiting especially when there aren't measurements close to the source.

Practical issues that warrant further investigation include the sensitivity of the results to changes in the model. Similarly, ability to singularly distinguish the source can be an issue when the correlations associated with different locations are very similar. In both cases, light inaccuracies in the model and/or close correlations, we would like to identify a set of buses in a region for which we have confidence includes the source of oscillation. We presented a pairwise-analysis of closeness. Further examination of these calculations should identifies regions in distinguishability.

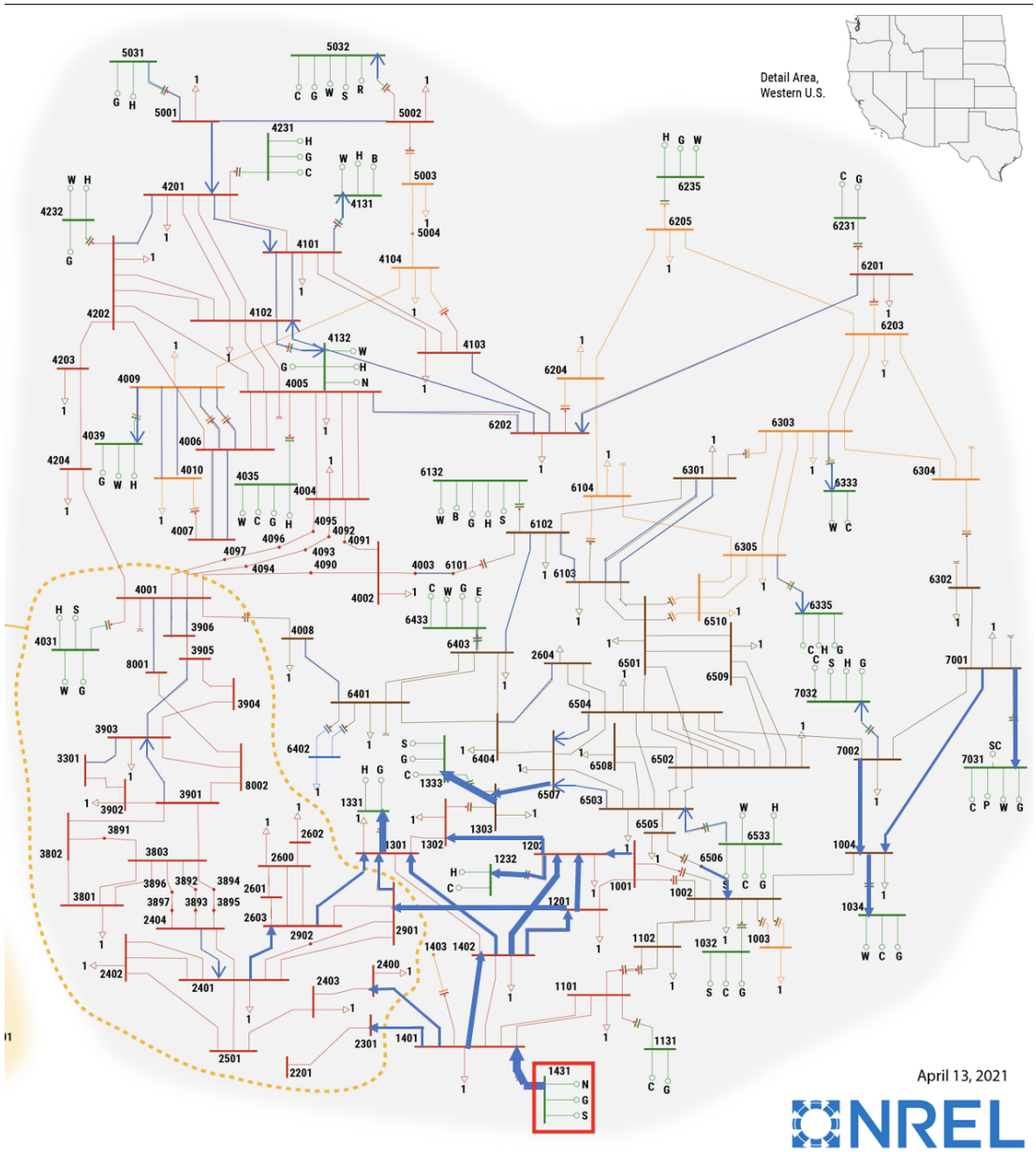

Fig. 3. Dissipated Power Within Case 1 of the NASPI Competition

Acknowledgement

The authors gratefully acknowledge support for this work through DOE ARPA-E project DE-AR0001032.

References

[1] Bin Wang and Kai Sun. Location methods of oscillation sources in power systems: a survey. *Journal of Modern Power Systems and Clean Energy*, 5(2):151–159, 2017.

[2] Ning Zhou. A coherence method for detecting and analyzing oscillations. In *2013 IEEE Power Energy Society General Meeting*, pages 1–5, 2013.

[3] Jim Follum and John W. Pierre. Initial results in the detection and estimation of forced oscillations in power systems. In *2013 North American Power Symposium (NAPS)*, pages 1–6, 2013.

[4] Francisco P Demello and Charles Concordia. Concepts of synchronous machine stability as affected by excitation control. *IEEE Transactions on power apparatus and systems*, 88(4):316–329, 1969.

[5] Q Wang, Y Min, and Y Zhang. Electrical torque analyses in multi-machine power systems. *JOURNAL-TSINGHUA UNIVERSITY*, 48(1):9, 2008.

[6] Yanghai Li, Ying Huang, Ju Liu, W Yao, and J Wen. Power system oscillation source location based on damping torque analysis. *Power system protection and control*, 43(14):84–91, 2015.

[7] Yi Gao, Di-chen Liu, Guan-bin Huang, and Qiu-yun Shi. Locating method of disturbance source of forced power oscillation based on prony anyasis. In *2012 China International Conference on Electricity Distribution*, pages 1–4. IEEE, 2012.

[8] Slava Maslennikov, Bin Wang, Qiang Zhang, auFeng Ma, auXiaochuan Luo, auKai Sun, and Eugene Litvinov. A test cases library for methods locating the sources of sustained oscillations. In *2016 IEEE Power and Energy Society General Meeting (PESGM)*, pages 1–5, 2016.

[9] N Al-Ashwal, D Wilson, and M Parashar. Identifying sources of oscillations using wide area measurements. In *Proceedings of the CIGRE US National Committee 2014 grid of the future symposium, Houston*, volume 19, 2014.

[10] WANG Maohai and SUN Hao. An analysis method for forced power oscillation source detection [j]. *Proceedings of the CSEE*, 34(34):6209–6215, 2014.

[11] Ryan B Myers and Daniel J Trudnowski. Effects of forced oscillations on spectral-based mode-shape estimation. In *2013 IEEE Power & Energy Society General Meeting*, pages 1–6. IEEE, 2013.

[12] S Arash Nezam Sarmadi and Vaithianathan Venkatasubramanian. Inter-area resonance in power systems from forced oscillations. *IEEE Transactions on Power Systems*, 31(1):378–386, 2015.

[13] Lei Chen, Yong Min, and Wei Hu. An energy-based method for location of power system oscillation source. *IEEE Transactions on Power Systems*, 28(2):828–836, 2013.

[14] Slava Maslennikov, Bin Wang, and Eugene Litvinov. Dissipating energy flow method for locating the source of sustained oscillations. *International Journal of Electrical Power Energy Systems*, 88:55–62, 2017.

[15] Slava Maslennikov and Eugene Litvinov. Iso new england experience in locating the source of oscillations online. *IEEE Transactions on Power Systems*, 36(1):495–503, 2021.

[16] Yuan Zhi and Vaithianathan Venkatasubramanian. Analysis of energy flow method for oscillation source location. *IEEE Transactions on Power Systems*, 36(2):1338–1349, 2021.

[17] Urmila Agrawal, John W. Pierre, Jim Follum, Dongliang Duan, Daniel Trudnowski, and Matt Donnelly. Locating the source of forced oscillations using pmu measurements and system model information. In *2017 IEEE Power Energy Society General Meeting*, pages 1–5, 2017.

[18] Jin Ma, Pu Zhang, Hong-jun Fu, Bo Bo, and Zhao-yang Dong. Application of phasor measurement unit on locating disturbance source for low-frequency oscillation. *IEEE Transactions on Smart Grid*, 1(3):340–346, 2010.

[19] Han Wu, Qingang Duan, and Jin Ma. Disturbance source self-diagnosis of the smart grid. In *2012 Spring Congress on Engineering and Technology*, pages 1–4. IEEE, 2012.

[20] Changjiang Jiang, Junyong Liu, Youbo Liu, J Gou, C Chen, R Chen, and M Bazargan. Online forced oscillation detection and identification based on wide area measurement system and cell theory. *Electric Power Automation Equipment*, 35(2):125–132, 2015.

[21] Thomas R Nudell and Aranya Chakrabortty. Graph-theoretic methods for measurement-based input localization in large networked dynamic systems. *IEEE Transactions on Automatic Control*, 60(8):2114–2128, 2015.

[22] Sandip Roy, Wenyun Ju, Neeraj Nayak, and Bernard Lesieutre. Localizing power-grid forced oscillations based on harmonic analysis of synchrophasor data. In *2021 55th Annual Conference on Information Sciences and Systems (CISS)*, pages 1–5, 2021.

[23] 2021 ieee-naspi oscillation source location contest. http://web.eecs.utk.edu/∼kaisun/Oscillation/2021Contest/. Accessed: 2022-07-08.

[24] DSA Tools. *Powerflow Short-circuit Analysis Tool User Manual*. PowerTech Labs Inc., Surrey, British Columbia Canada, 2021.

[25] DSA Tools. *Transient Security Assessment Tool User Manual*. PowerTech Labs Inc., Surrey, British Columbia Canada, 2021.

[26] DSA Tools. *Small Signal Analysis Tool User Manual*. PowerTech Labs Inc., Surrey, British Columbia Canada, 2021.